Rare Metal Materials and Engineering
Volume 53, Issue 4, April 2024
Available online at www.rmme.ac.cn

Science Press

Cite this article as: Jin Lan, Li Kaiqiang, Yi Tinghua. Effect of Loading Temperature on Processed Surface of Ni_3Al-Based Alloy by MD Simulation[J]. Rare Metal Materials and Engineering, 2024, 53(04): 1011-1020. DOI: 10.12442/j.issn.1002-185X.20230552.

ARTICLE

Effect of Loading Temperature on Processed Surface of Ni_3Al-Based Alloy by MD Simulation

Jin Lan[1,2], Li Kaiqiang[1,2], Yi Tinghua[1,2]

[1] School of Mechanical and Electrical Engineering, Lanzhou University of Technology, Lanzhou 730050, China; [2] Engineering Research Center of New Nonferrous Metallurgy Equipment, Ministry of Education, Lanzhou University of Technology, Lanzhou 730050, China

Abstract: In order to enhance the nano-cutting surface quality of Ni_3Al-based alloy to obtain better service state, the nano-molecule dynamics (MD) simulation and micro-cutting experiment were combined to investigate the effect of loading temperature (300–1050 K) on cutting force and surface morphology. MD simulation results show that the fluctuation of cutting force is the smallest when the loading temperature is 750 K during nano-cutting process of Ni_3Al-based alloy, compared with that at other temperatures. When the loading temperature is 600–750 K, the number of convex atoms affecting the surface morphology is the least, which indicates that Ni_3Al-based alloy can achieve higher surface quality at loading temperature of about 750 K. The micro-cutting experiments of Ni_3Al-based alloy show that higher flatness of the processed surface can be obtained at the loading temperature of 600–750 K, which indirectly verifies the feasibility of MD simulation results of the nano-cutting process of Ni_3Al-based alloy. Results suggest that selecting appropriate loading temperature is an effective method to improve the nano-cutting surface quality of Ni_3Al-based alloy.

Key words: Ni_3Al-based alloy; nano-cutting; processed surface; loading temperature; molecular dynamics simulation; micro-cutting experiment

As the indispensable alloys in aerospace and high-end manufacture fields, Ni-based superalloys become more and more widely used[1], and their performance accounts for about 40% of the comprehensive material quality for aero-engines[2]. Because Ni-based superalloys are mainly γ-Ni_3(Al, Ti) metal compounds, they have higher high-temperature strength than the iron/cobalt-based superalloys do, and they also have better resistance against oxidation and corrosion, ensuring the excellent performance in complex high-temperature environments[3–8]. These characteristics contribute to their wide application but result in the processing difficulties. It is found that in the nano-cutting process, Ni_3Al-based alloy has high hardness (caused by the microstructure strengthening phase), high shear stress resistance, low thermal conductivity (easily leading to large cutting force), and high cutting temperature, resulting in serious tool wear[9–12]. Therefore, it is necessary to improve the processing quality of Ni_3Al-based alloy to ensure the stable and reliable work in extremely harsh environments, such as high temperature and high pressure.

The essence of nano-cutting process is to destroy the binding energy between atoms for the workpiece atom removal, which enables the material to be processed at nanometer scale, effectively increasing the machining accuracy of the workpiece. Tian et al[13–14] simulated the nano-cutting process of Ni_3Al single crystal and found that the shape of cutting groove on the workpiece surface has a wide front and a narrow back. During the nano-cutting process, the workpiece temperature and system potential energy gradually increase, but the elastic recovery and lattice reconstruction of machined surface may weaken the increasing rate of temperature and system potential energy. Fan et al[15] used CBN tool to cut the Ni-based alloy containing γ' phase (Ni_3Al) and found that the grain boundary atoms of workpiece are the easiest to diffuse under cutting action, followed by the phase boundary atoms. The lattice atoms are the most difficult to diffuse. When the workpiece atoms are diffused into the tool, they are prone to move to the grain boundary, rather than to form interstitial impurity atoms or to displace impurity

Received date: September 04, 2023
Foundation item: Key Research and Development Project of Gansu (21YF5GA080)
Corresponding author: Li Kaiqiang, Master, School of Mechanical and Electrical Engineering, Lanzhou University of Technology, Lanzhou 730050, P. R. China, E-mail: LKQlikaiqiang@163.com

atoms. Feng et al[16] compared the subsurface damage and surface roughness of Ni_3Al single crystal after nano-cutting with different tool rake angles. It is found that chip thickness gradually increases. The subsurface damage is decreased with increasing the tool rake angle. A regular slip surface is formed in front of the tool, and the surface is smoother when the tool rake angle is 30°, compared with that with other tool rake angles.

Ni_3Al-based alloy has the "R" phenomenon when the temperature is lower than 1173 K[17–20]: its yield strength is increased with increasing the temperature in a specific temperature range, but it is decreased rapidly with further increasing the temperature over the peak temperature. Therefore, Ni_3Al-based alloys have been used for tool manufacture and show great potential[21–23]. Ni_3Al-based alloys can generate more cutting heat during the cutting process and their thermal conductivity is low[24]. When the cutting temperature is in the "R" phenomenon temperature range, the yield strength of Ni_3Al-based alloys is high and the machined surface quality is inferior. Since the Ni_3Al-based alloy structure remains orderly until the temperature reaches the melting point (1668 K)[18], the loading temperature of Ni_3Al-based alloy workpiece can be altered, which lowers the hardness of cutting area at high temperature, therefore improving the processing quality.

The influence of cutting temperature on the machining quality of materials has also been widely studied. Jiang et al[25] used the finite element method to simulate the laser heating-assisted cutting process of beryllium materials and verified that the laser heating-assisted machining method can better improve the surface machining quality of the materials by comparing the instantaneous interface diagrams at molecular dynamics (MD) microscopic cutting state in the cutting experiments. Luo et al[26] studied the effects of different loading temperatures on the cutting process of single crystal germanium and found that the cutting force is decreased with increasing the cutting temperature, and the number of workpiece atoms under lattice transformation is increased. Chavoshi et al[27–28] studied the nano-cutting process of 3C-SiC at high loading temperature and found that the subsurface damage is increased linearly with increasing the cutting temperature. When the thermal energy is high enough, point defects are generated, and the higher the loading temperature, the faster the stacking fault growth on the sliding surface. Shao et al[29] analyzed the surface quality changes of single crystal γ-TiAl alloy after nano-cutting process under low temperature loading. It is concluded that the optimal loading temperature is 173 K and the cohesive energy of single crystal γ-TiAl alloy increases at low temperature. However, the effect of loading temperature on the surface quality of Ni_3Al-based alloy during nano-machining process is rarely reported, which restricts the development of Ni_3Al-based alloys.

Currently, MD simulation has become an important tool for micro-scale investigations. In MD simulation, it is assumed that the motion of particles follows the classical mechanics or quantum mechanics laws. By solving the motion equations of each interacting particle, the trajectory of all particles in the system of phase space can be obtained, and then the macroscopic physical characteristics of the overall system can be obtained according to statistical mechanics[30].

This research investigated the effect of loading temperature on surface quality of Ni_3Al-based alloy at the beginning of nano-cutting process by MD simulation. In order to verify the simulation results, the micro-cutting experiments of Ni_3Al-based alloy were designed and conducted. This research provided theoretical basis to improve the machinability of Ni_3Al-based alloys.

1 MD Simulation Modeling

The Ni_3Al-based alloy used in this research was $L1_2$-type face-centered cubic (fcc) alloy with lattice constant of a= 0.3572 nm, and its schematic diagram is shown in Fig.1. Due to the small depth of nano-cutting process and the efficiency of computer simulation, the model size should not be too large. In this research, the Ni_3Al-based alloy workpieces were constructed by periodically arranging the lattices in three-dimensional (3D) space. The model size was $65a \times 30a \times 20a$ and contained 159 820 atoms. The crystal orientations were x-[100], y-[010], and z-[001], and the cutting direction was the $[\bar{1}00]$ of the (010) surface. The workpiece was divided into Newton layer, thermostat layer, and boundary layer. In order to prevent the loss of chip atoms during nano-cutting process, free boundary conditions were adopted in the x and y directions. Selecting periodic boundary conditions in the z direction was equivalent to construct a quasi-infinite workpiece, which could more truly reflect the actual working conditions and reduce the influence of size effect. All simulations in this research were based on the MD codes of large-scale atomic/molecular massively parallel simulator (LAMMPS[31]) software to study the loading temperature. According to the simulation results, OVITO[32] was used to analyze and visualize the atomic position.

The atomic potential function plays a key role in MD simulation. The correct selection of the potential function between atoms and the potential parameters in potential function is the basis to ensure the accuracy of MD simulation results. In this research, the empirical potential function was used to describe the interaction between Ni_3Al workpiece (Ni-Al) and diamond tool (C-C) atoms. The selection results are shown in Table 1.

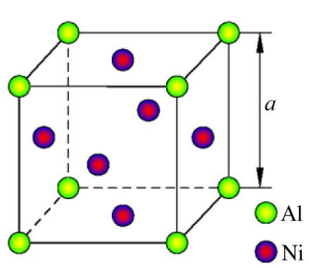

Fig.1 Schematic diagram of cell structure of Ni_3Al-based alloy

Table 1 Selection results of potential function

Atom type	Potential function
Diamond tool (C-C)	SiC_1994.tersoff[33]
Workpiece and cutting tool	Mishin-Ni-Al-2009.eam.alloy[34]
Workpiece (Ni-Al)	Morse potential

Tersoff potential was used to describe the C-C interactions between tool atoms. The embedded atom potential (EAM) was used to describe the Ni-Al interactions between atoms. The interaction between workpiece and tool atoms was described by Morse potential, and the parameters of Morse potential function are shown in Table 2.

Diamond tools have extremely high hardness and wear resistance, which can improve the processing quality of workpiece[35–36], so they are commonly used in nano-cutting machining. Diamond tools are prone to oxidation and graphitization in high temperature environment, but the mechanisms are different in different media[37]. When the temperature reaches 1123 K, diamond starts to oxidize in the air, but graphitization does not occur in vacuum and inert gas when the temperature is below 1773 K[38]. Because the environment of the simulation process in this research was vacuum, the diamond tool was applicable under the condition of high temperature loading.

3D MD nano-cutting model consisted of Ni_3Al workpiece and diamond tools, as shown in Fig.2. The specific simulation parameters and boundary conditions of Ni_3Al workpiece are shown in Table 3. Appropriate distance between the workpiece and the tool should be retained. If the distance is too small, the gravitational effect may occur between the workpiece atom and the tool atom. If the distance is too large, the computing resources are wasted. Therefore, the distance was set as 2 nm in this MD simulation.

2 MD Simulation Analysis

According to the parameters in Table 3, the applicable loading temperature range was determined by analyzing the changes of cutting temperature, cutting force, and processed surface topography under different loading temperatures.

Table 2 Morse potential function parameters

Interaction	D/eV	α/nm^{-1}	r/nm
Ni-C	1.003 92	19.874 5	0.261 994
Al-C	0.469 1	17.38	0.224 6

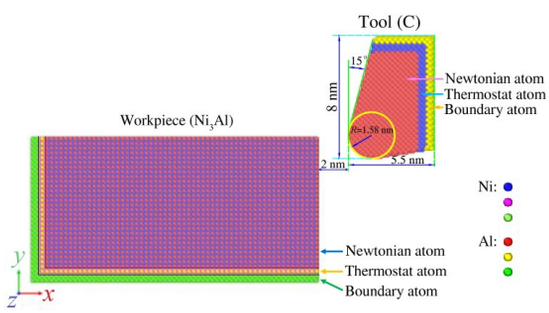

Fig.2 Schematic diagram of MD simulation model

Table 3 MD simulation parameters of fcc Ni_3Al workpiece

Parameter	Value
Workpiece size	65a×30a×20a (a=0.3672 nm)
Arc radius of tool tip/nm	1.58
Rake and back angle/(°)	15, 6
Boundary condition	ssp
Time step/ps	0.001
Cutting depth/nm	1.5
Cutting length/nm	20
Cutting speed/nm·ps^{-1}	0.1
Loading temperature/K	300, 450, 600, 750, 900, 1050

2.1 Cutting temperature

In MD simulation of nano-cutting process of Ni_3Al-based alloy under high temperature loading, the heat mainly comes from two directions: (1) the heat caused by loading temperature, which is the heat of workpiece before the nano-cutting process; (2) the cutting heat, which is released by the change and destruction of the workpiece atom lattice under the action of tool. The combined effect of loading temperature and cutting heat leads to the change of cutting temperature of Ni_3Al-based alloy workpiece. Through cutting simulation, the average atomic temperature distribution of the workpiece on the xy plane at cutting distance of 15 nm is obtained, as shown in Fig.3.

According to the temperature distribution of Ni_3Al-based alloy workpiece at different loading temperatures in Fig. 3, it can be found that the atomic temperature at the chip is much higher than that inside the workpiece. The distribution of atoms with higher temperature in the workpiece begins to expand from the contact area with the tool to the inside area of the workpiece, and the diffusion area is gradually increased with increasing the loading temperature, which indicates that the high temperature atoms in the nano-cutting process of Ni_3Al-based alloy workpiece are mainly distributed around the tool. The mean value of the atom temperature of the workpiece around the tool is used as the cutting temperature, and its change with the loading temperature is shown in Fig.4. Loading temperature and cutting temperature present the same upward variation trends. However, with increasing the loading temperature to 600 – 900 K, the increasing rate of cutting temperature becomes slower, indicating that the heat generated during the nano-cutting process has a little effect on the flatness of the workpiece surface.

2.2 Cutting force

As shown in Fig. 5a, with the nano-cutting process proceeding, the total cutting force (F_r), tangential force (F_x), and normal force (F_y) of the Ni_3Al-based alloy workpiece during the nano-cutting process are firstly increased and then remain stable with fluctuations, whereas the lateral force (F_z) fluctuates around 0 the whole time. F_x and F_r have similar variation trends in the nano-cutting process. Therefore, F_x is

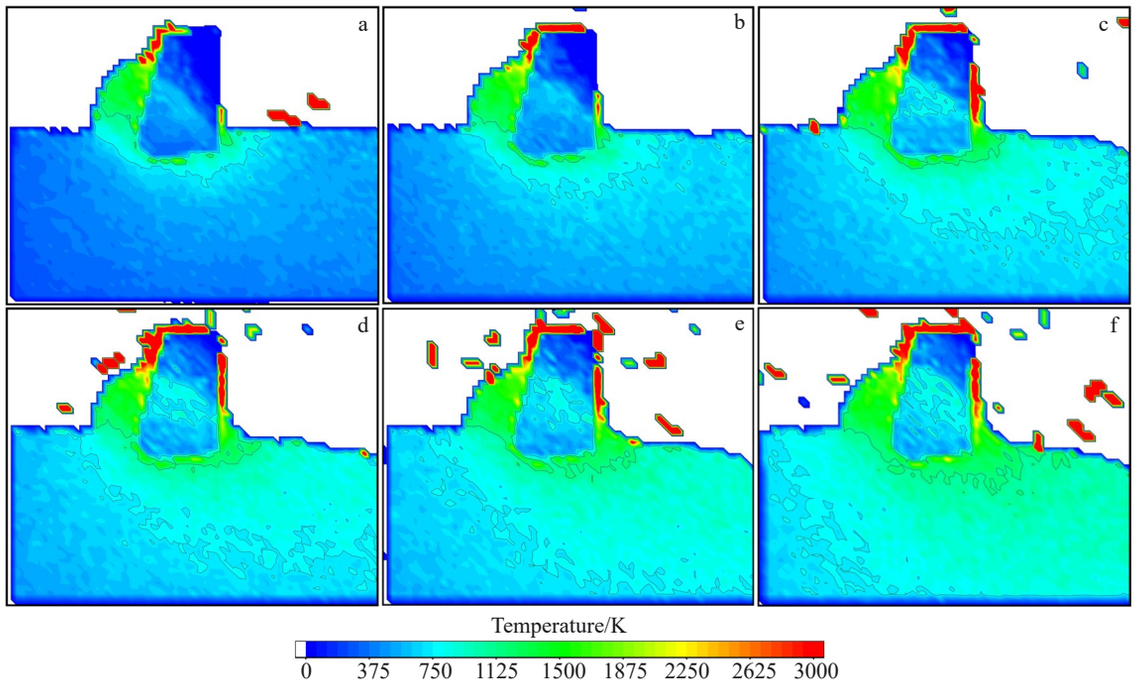

Fig.3 Temperature distributions of Ni_3Al-based alloy workpiece at different loading temperatures and cutting distance of 15 nm: (a) 300 K, (b) 450 K, (c) 600 K, (d) 750 K, (e) 900 K, and (f) 1050 K

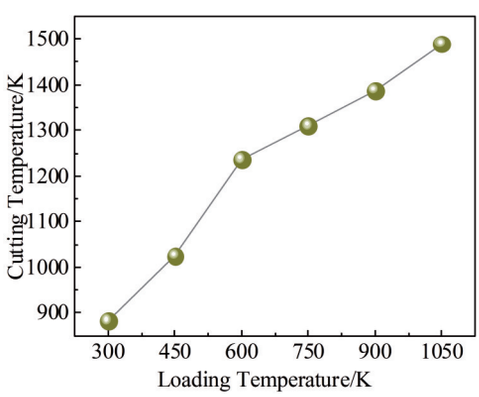

Fig.4 Variation of cutting temperature with loading temperature

taken as the main influence factor besides loading temperature.

As shown in Fig. 5b, the cutting force data with large deviation, which are marked by the red boxes, are removed to obtain the extreme values $F_{x_{max}}$ and $F_{x_{min}}$ of remaining cutting force. The polynomial fitting curve of the cutting force data is obtained and then the average cutting force ($F_{x_{ave}}$) of the workpiece in the stable cutting stage can be calculated.

Therefore, ΔF_x at different loading temperatures in the nano-cutting process of Ni_3Al-based alloy can be obtained by $\Delta F_x = |F_{x_{max}} - F_{x_{min}}|$, where ΔF_x presents the difference between two extreme values of the stable cutting force, indicating the fluctuation of cutting force.

As shown in Fig.6, in the temperature range of 300–750 K, $F_{x_{ave}}$ and ΔF_x are firstly increased and then decreased with increasing the loading temperature, reaching the maximum cutting force at 600 K. ΔF_x reaches the lowest value at 750 K,

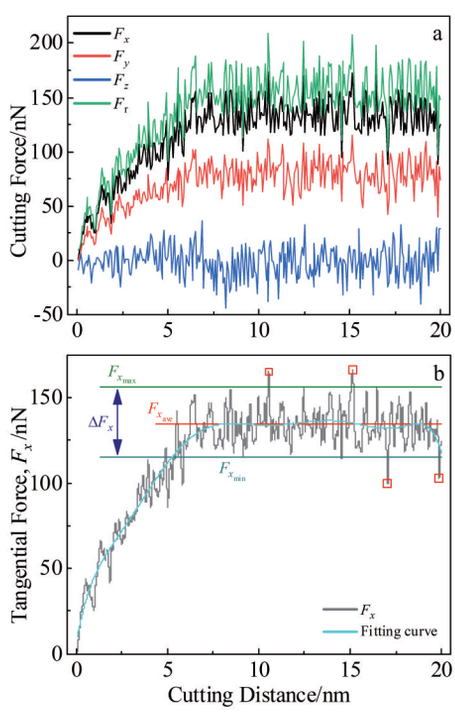

Fig.5 Variation of cutting force (a) and tangential force (b) during nano-cutting process of Ni_3Al-based alloy workpiece

indicating that the surface flatness can be better processed at this loading temperature. When the loading temperature exceeds 750 K, $F_{x_{ave}}$ continues to decline and ΔF_x increases sharply, indicating that the fluctuation of cutting force increases and the corresponding machined surface becomes uneven.

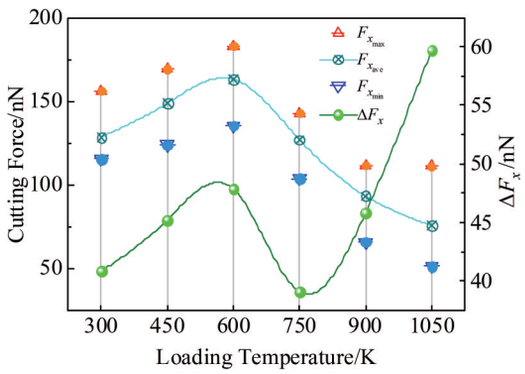

Fig.6 Variations of $F_{x\max}$, $F_{x\min}$, $F_{x\text{ave}}$, and ΔF_x with loading temperature

Combined with Fig. 4, the main reason for the abovementioned phenomena is that when the loading temperature is lower than 600 K, the yield strength of Ni_3Al-based alloy workpiece is increased with increasing the loading temperature. Thus, the cutting force increases and the fluctuation of cutting force increases accordingly. When the loading temperature exceeds 600 K, the cutting temperature of Ni_3Al-based alloy workpiece exceeds the temperature range of the "R" phenomenon and the yield strength decreases, so the cutting force decreases. When the loading temperature exceeds 900 K, the thermal softness of Ni_3Al-based alloy workpiece increases greatly and the lattice stability decreases under the stress state, so the fluctuation of cutting force increases significantly. In summary, when the loading temperature is 750 K, the cutting force and cutting force fluctuation are small, indicating that the nano-cutting process is stable and the quality of machined surface is optimal.

2.3 Surface topography

The flatness of the machined surface depends on the concave and convex states of the surface atoms in the nanoscale. Due to the destruction of lattice arrangement in the cutting zone during the nano-cutting process, the structure of the rebound part of the lattice is restored during the cooling process of workpiece to room temperature after the cutting is completed. However, there are still a lot of atoms disorderly arranged on the machined surface, resulting in the appearance of different concave and convex defects. After the Ni_3Al-based alloy workpiece is cooled to room temperature, the atoms in *y*-direction (cutting depth direction) of the machined surface are presented in Fig.7.

Because the concave and convex conditions of the machined surface cannot be clearly observed in Fig. 7, the schematic diagram of concave and convex of machined surface is presented in Fig.8. The atoms in the convex area of the machined surface are regarded as A-type ones, and the atoms in the concave area are regarded as V-type ones. The more the A-type atoms, the more severe the protrusion of the machined surface; the less the V-type atoms, the more severe the depression of the machined surface.

Fig. 9 shows the variations of the number of atoms in convex and concave areas on the machined surface at different

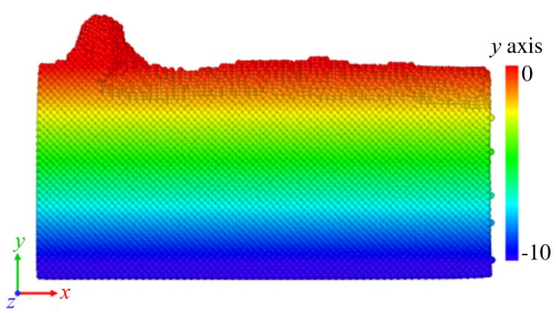

Fig.7 Atom distribution of machined surface in *y*-direction after cooling process

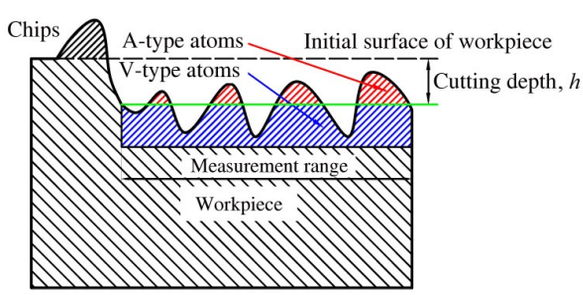

Fig. 8 Schematic diagram of concave and convex of machined surface

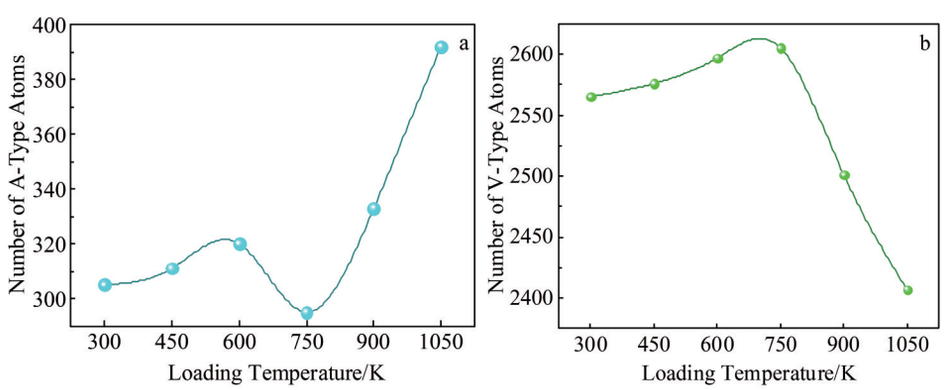

Fig.9 Variations of the number of atoms in convex (a) and concave (b) areas on machined surface with loading temperatures

loading temperatures. The cutting depth is set based on the measurement method in Fig. 8, which is the thickness of two layers of atoms under the surface layer. As shown in Fig. 9a, the number of A-type atoms is increased firstly and then decreased with increasing the loading temperature from 300 K to 750 K, reaching the minimum value at the loading temperature of 750 K. Then, the number of A-type atoms is increased rapidly with further increasing the loading temperature. Therefore, the number of A-type atoms on the machined surface is the smallest at the loading temperature of 750 K. The variation trend of the number of A-type atoms is similar to that of the cutting force fluctuation in Fig. 6. This phenomenon can be attributed to the fact that Ni_3Al-based alloy belongs to the $L1_2$-type metal compound, who has the "R" phenomenon. Therefore, the yield strength is increased with increasing the loading temperature within this specific range. When the loading temperature exceeds the peak temperature, the yield strength decreases rapidly.

For the Ni_3Al-based alloy, when the loading temperature is lower than 600 K and the cutting temperature is below 1250 K, the yield strength of the workpiece is increased with increasing the loading temperature. Thus, the required cutting force also increases, so does the number of A-type atoms. With increasing the loading temperature from 600 K to 750 K, the yield strength of Ni_3Al-based alloy is decreased. Therefore, the required cutting force decreases, and the A-type atoms also decrease. However, when the loading temperature exceeds 900 K, the thermal flexibility of the workpiece increases greatly and the lattice stability decreases under the stress. Therefore, the fluctuation of cutting force increases significantly, and the number of A-type atoms also increases.

As shown in Fig. 9b, the number of V-type atoms is increased slowly and decreased rapidly with increasing the loading temperature to 750 K. When the loading temperature is lower than 750 K, the depression degree of the workpiece barely changes. When the loading temperature is between 600 and 750 K, the surface depression is the least obvious. However, when the loading temperature exceeds 750 K, the surface depression is obviously aggravated. Moreover, the variation trend of the number of V-type atoms is similar to that of the mean cutting force in Fig. 6. These phenomena also indicate that the size and fluctuation of cutting force have a certain impact on the surface quality of the workpiece.

Comparing the variation ranges of the number of A-type and V-type atoms, it can be found that the variation range of the number of V-type atoms is significantly higher than that of A-type atoms, indicating that the concave defects are more than the convex defects on the machined surface. This is mainly because the force of the tool atoms on the workpiece atoms during machining causes damage to the atomic structure of the machined surface, and some atoms with severe structural damage are attached to the tool by the gravitational force of the tool atoms. In this case, the depression of this part is aggravated, and the cutting depth is also increased when the workpiece atoms are attached to the tool bottom, which further aggravates the depression defect.

Combined with Fig. 4, Fig. 6, and Fig. 9, it can be seen that when the loading temperature is lower than 900 K, the fluctuation of cutting force is small, and the concave-convex phenomena on the machined surface of Ni_3Al-based alloy workpiece are less obvious. When the loading temperature is 750 K and the cutting temperature is 1300 K, the number of convex and concave defects on the machined surface is the least, and the fluctuation of cutting force is the smallest. Therefore, in order to ensure the processed surface quality of workpiece, the loading temperature should be controlled at about 750 K.

3 Experiment

The size of the Ni_3Al-based alloy specimen was (5.0±0.1) mm×(5.0±0.1) mm, and the thickness was (1.0±0.05) mm. Because the scratches generated by the cutting experiments were tiny and the requirement of workpiece surface accuracy was high, the machining surface was polished to obtain the workpiece with surface roughness R_a<0.01 μm, as shown in Fig.10.

The Ni_3Al-based alloy workpiece used in the experiment was processed by MFT-5000 Multi-Function Tribometer (Rtec-instruments) with natural diamond Rockwell indenter. The temperature environment chamber maintained the internal temperature as 273 – 973 K, and the inert gas was used to improve the thermal stability of tool[37–38]. The 3D optical profiler Zygo NV7300 was selected as the surface inspection equipment and the test data were extracted by ZYGO MetroPro® software.

Nano-scale machining is difficult to achieve in experiments, and the current nano-processing experiments mainly focus on the nano-imprint technique. Due to the restrictions of workpiece surface roughness and machining instruments, the cutting experiments in this research could only be conducted at the micron level, and the nano-cutting process was simulated by the scratch motion of the indenter. Therefore, quantitative analysis of the simulation could not be achieved. Only the qualitative analysis could be achieved.

In the experiments, the cutting depth could not be controlled directly, and it was controlled by the load. The load applying methods have two types. One is the constant force loading: the indenter is applied with a fixed normal load, and the workbench completes the cutting experiment with the

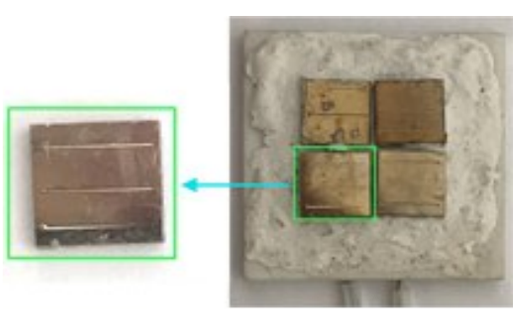

Fig.10 Appearances of experiment specimens

specimens moving continuously along a certain direction. The other is variable force loading, which applies a variable normal load to the indenter with the workbench moving. In this experiment, the normal load was determined by variable force loading method.

Fig.11 shows the relationship between the cutting depth and normal load at different cutting distances during the variable force loading process at loading temperature of 300 K. It can be seen that the applied normal load is increased with increasing the cutting depth. When the cutting depth is 10 μm, the required normal load is 25 N, so the constant force loading method with normal load of 25 N was adopted in the further experiments. According to the MD simulation results of Ni_3Al-based alloy after nano-cutting process at the actual conditions, the cutting experiment scheme was designed, as listed in Table 4.

Through the analysis of experimental results, the influence of loading temperature on workpiece machining surface and cutting force during the nano-cutting process was investigated. The morphology of cutting surface was obtained by ZYGO MetroPro® software, as shown in Fig. 12. In order to analyze the machining quality of the cutting surface, the surface profile height was measured along the cutting direction during the steady cutting stage. The profile heights of the cutting surface at different loading temperatures are shown in Fig. 13. The red line is the average contour height of the measured part (h_{ave}); the maximum height (h_{max}) and the minimum height (h_{min}) of the measured part are marked by green and cyan lines, respectively; the difference (Δh) between the highest and lowest contour point is also marked. The surface profile height is the distance from the unprocessed surface, so the height value is negative, which indicates that the larger the absolute value of surface profile height, the larger the cutting depth.

Table 4 Cutting experiment parameters

No.	Loading temperature/K	Normal load/N	Cutting speed/ $mm \cdot s^{-1}$
1	300	25	0.1
2	750	25	0.1
3	900	25	0.1

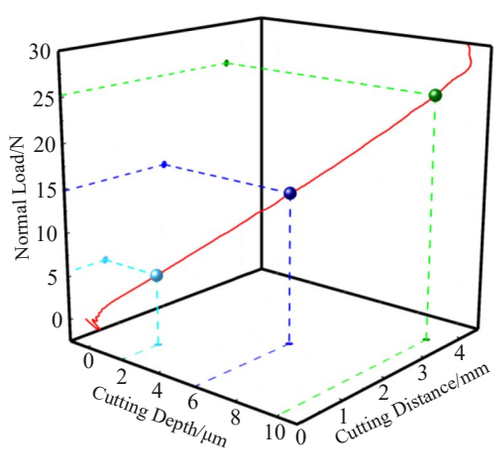

Fig.11 Relationship between cutting depth and normal load at different cutting distances

It can be seen from Fig. 13 that the profile height of the workpiece cutting surface fluctuates near the mean value at different loading temperatures, which can reflect the unevenness of the workpiece surface. The greater the difference between the two extreme values of the surface profile height, the worse the flatness of the workpiece surface. The h_{ave}, h_{max}, h_{min}, and Δh of the measured part are obtained from Fig. 13, and the variation of the surface profile height with loading temperature is described, as shown in Fig. 14. As shown in Fig. 14, with increasing the loading temperature, the surface profile height of the workpiece is decreased, the cutting depth is increased, and the difference of surface profile height is firstly decreased and then increased rapidly. In a certain loading temperature range, the hardness of Ni_3Al single crystal is positively correlated with the temperature change. Under the same normal load, the cutting depth is increased with increasing the loading temperature, indicating that when the loading temperature reaches 750 K, the hardness begins to decrease with increasing the cutting temperature. As shown in Fig. 14, the difference of surface profile height is slightly smaller at the loading temperature of 750 K than that at the loading temperature of 300 K, indicating that the machined surface quality is higher at the loading temperature of 750 K. When the loading temperature rises to 900 K, the difference of surface profile height increases rapidly, indicating that the machined surface quality is inferior.

When the loading temperature is 300 K, the variation of

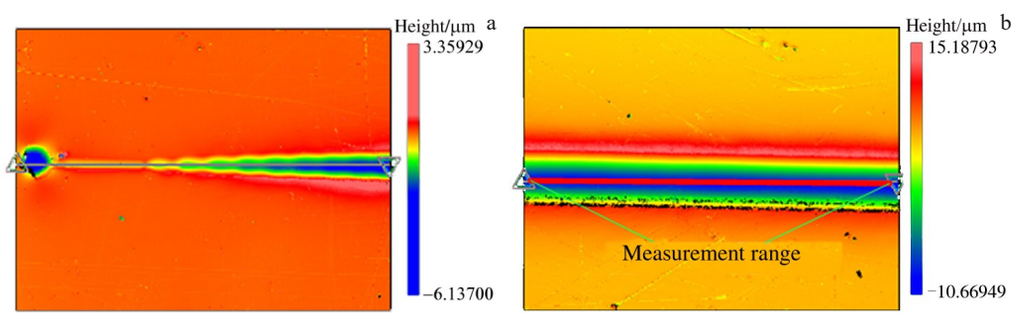

Fig.12 Contour maps of cutting surface at initial stage (a) and stable stage (b)

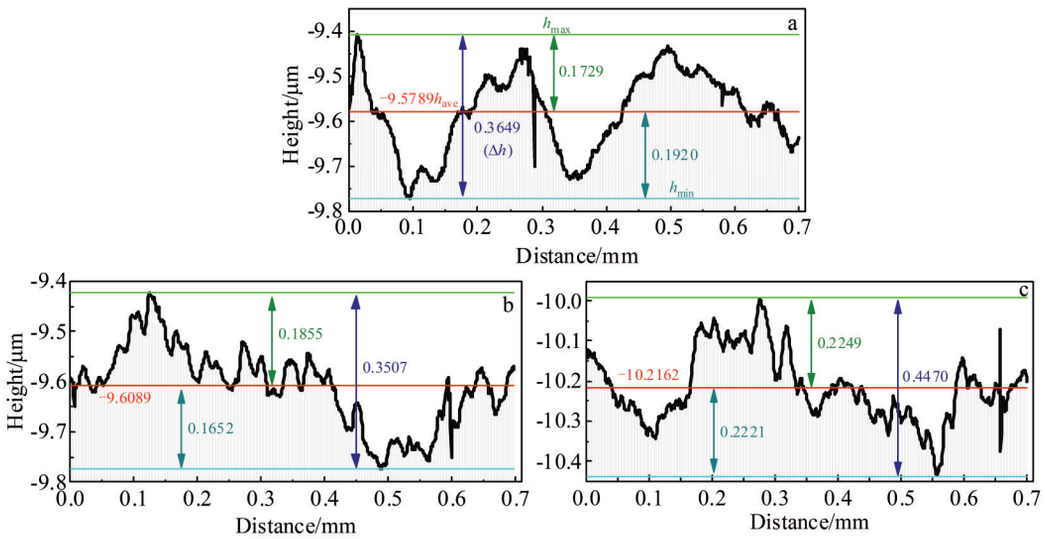

Fig.13 Cutting surface profiles at loading temperatures of 300 K (a), 750 K (b), and 900 K (c)

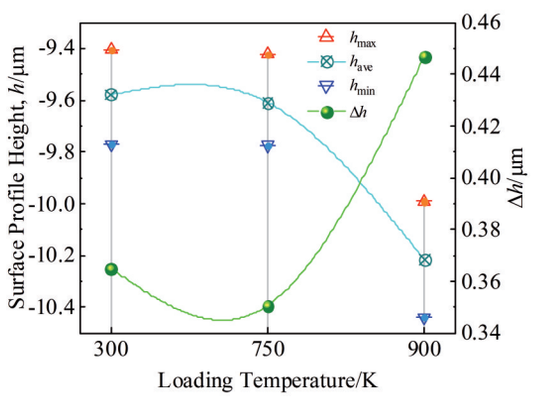

Fig.14 Variation of surface profile height with loading temperatures

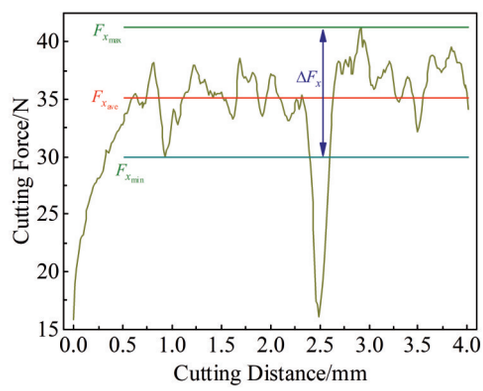

Fig.15 Variation of cutting force in nano-cutting process at loading temperature of 300 K

tangential force in the nano-cutting process is shown in Fig. 15. Similar to the variation of tangential force in Fig. 5b, with the nano-cutting process proceeding, the cutting force is increased gradually and then fluctuated around a stable value. Affected by the quality of tool and workpiece, the cutting force fluctuates greatly at the cutting distance of 2.5 mm. Except the large fluctuations of the cutting force data, F_{xave} is used to represent the cutting force under this loading temperature, and ΔF_x is used to represent the fluctuation of cutting force. Fig. 16 shows the effect of different loading temperatures on the cutting force. It can be seen that the cutting force is decreased with increasing the loading temperature. The difference of cutting force is small when the loading temperature is 300 and 750 K, and then the cutting force is decreased rapidly with further increasing the loading temperature. The fluctuation of cutting force is decreased firstly and then increased with increasing the loading temperature. This is because the hardness of Ni_3Al-based alloy is positively correlated with the temperature change within a certain loading temperature range. When the loading temperature is 750 K, the cutting temperature exceeds the peak temperature of "R" phenomenon. At this time, the

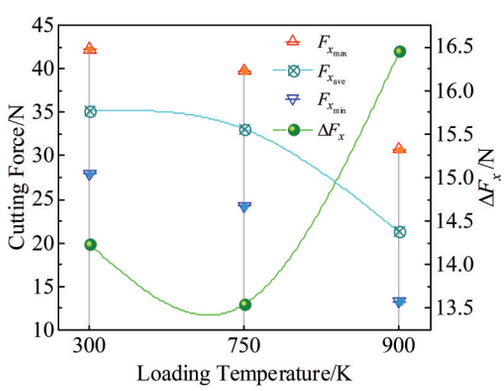

Fig.16 Variation of cutting force with loading temperatures

hardness is slightly smaller than that at the loading temperature of 300 K. Still, the cutting forces with loading temperature of 300 and 750 K are similar. When the loading temperature is 900 K, the hardness of workpiece decreases obviously due to the temperature, and the internal structure is unstable, which leads to the decrease in cutting force and the increase in cutting force fluctuation. The variation of cutting

force fluctuation also explains the change in the difference of surface profile height with loading temperature in Fig.14.

4 Comparative Analysis of Simulation and Experiment Results

Restricted by the surface roughness of workpiece and processing instrument, the order of magnitude of the cutting experiment was only at micron level, whereas the MD simulation was at the nanometer level.

Comparing Fig.9 with Fig.14, it can be seen that when the loading temperature exceeds 750 K, the surface roughness of the workpiece increases in the MD simulation and the actual cutting experiment, which is manifested by the sharp change of the convex and concave atoms and the increase in surface profile height. MD simulation and cutting experiment results both show that the high loading temperature can effectively improve the surface quality of Ni_3Al-based alloy under certain cutting parameters.

Comparing the variations of cutting force with loading temperature in Fig.6 and Fig.14, it can be seen that when the loading temperature exceeds 750 K, the cutting force shows an obvious downward trend and the fluctuation increases significantly. The direct result is that the corresponding machined surface is more uneven.

Through the comparative analysis of MD simulation and experiment results, it can be seen that the two results have high similarity, suggesting the feasibility of MD simulation in the study of Ni_3Al-based alloy during nano-cutting process.

5 Conclusions

1) MD simulation shows that the loading temperature and cutting force are the main influence factors of surface morphology. The cutting temperature rises gently when the loading temperature is 600 – 900 K, and the cutting force reaches the maximum with the loading temperature of 600 K, but the cutting force fluctuation reaches the minimum with the loading temperature of about 750 K. The number of convex atoms is the least when the loading temperature is about 750 K, and the processed surface has better surface flatness.

2) Compared with cutting experiments at room temperature, the surface flatness of the workpiece is improved, the cutting force fluctuation is smaller, and the processed surface quality is better when the loading temperature is 750 K, which indirectly verifies the MD simulation results and proves the enhancement feasibility of surface quality of Ni_3Al-based alloy after nano-cutting process by high loading temperature. In order to obtain better surface quality, the loading temperature should be controlled at about 750 K.

References

1 Wang Mingyang, Wang Bo, Cheng Yaonan *et al*. *Journal of Harbin University of Science and Technology*[J], 2015, 20(6): 24 (in Chinese)

2 Thakur A, Gangopadhyay S. *International Journal of Machine Tools and Manufacture*[J], 2016, 100: 25

3 Lin Dongliang. *Journal of Shanghai Jiao Tong University*[J], 1998, 32(2): 97 (in Chinese)

4 Zhang Rui, Liu Peng, Cui Chuanyong *et al*. *Acta Metallurgica Sinica*[J], 2021, 57(10): 1215 (in Chinese)

5 Fu Jiabo, Wang Chenchong, Mateo Carlos Gracia *et al*. *Materials China*[J], 2023, 42(9): 722 (in Chinese)

6 Nan Rong, Cai Jianhua, Yang Jian *et al*. *Titanium Industry Progress*[J], 2023, 40(5): 40 (in Chinese)

7 Yan H J, Tian S G, Dong Z F. *Rare Metal Materials and Engineering*[J], 2022, 51(1): 44

8 Sun J X, Liu J L, Chen C *et al*. *Rare Metal Materials and Engineering*[J], 2022, 51(2): 369

9 Zhou Y G, Gong Y D, Cai M *et al*. *International Journal of Advanced Manufacturing Technology*[J], 2017, 90(5–8): 1749

10 Liu Zhanqiang, Ai Xing. *Tool Engineering*[J], 2001, 35(12): 3 (in Chinese)

11 Song Zhiwei. *Tool Engineering*[J], 2000, 34(9): 23 (in Chinese)

12 Xia Z H, Gao B C, Yu J G *et al*. *Journal of Materials Research and Technology*[J], 2022, 19: 2447

13 Tian Jingjing, Liang Guoxing, Huang Yonggui *et al*. *Machinery Design & Manufacture*[J], 2021(7): 109 (in Chinese)

14 Tian Jingjing. *Simulation and Experimental Study on Machining Process of Ni_3Al Based Superalloy*[D]. Taiyuan: Taiyuan University of Technology, 2019 (in Chinese)

15 Fan Y H, Wang W Y, Hao Z P. *Proceedings of the Institution of Mechanical Engineers, Part B: Journal of Engineering Manufacture*[J], 2021, 235(11): 1763

16 Feng R C, Qi Y N, Zhu Z X *et al*. *International Journal of Precision Engineering and Manufacturing*[J], 2019, 21(5–6): 711

17 Chen Jinlu, Zhu Dingyi, Lin Dengyi. *Materials Reports*[J], 2006, 20(1): 35 (in Chinese)

18 Mei Bingchu, Wang Weimin, Yuan Runzhang. *Journal of Wuhan University of Technology*[J], 1996, 18(1): 1 (in Chinese)

19 Wang Xiaoming, Zhu Zuchang. *Heat Treatment*[J], 2010, 25(3): 6 (in Chinese)

20 Pawel J, Wojciech P, Zbigniew B. *Materials*[J], 2015, 8(5): 2537

21 Wei Xuelong, Zhang Jianjun, Liu Kaobin *et al*. *Cemented Carbides*[J], 2020, 37(5): 400 (in Chinese)

22 Han Xu. *Research on the Preparation and Cutting Performance of WC-Ni_3Al-Based Cemented Carbide Tool Materials*[D]. Xiangtan: Hunan University of Science and Technology, 2022 (in Chinese)

23 Cheng Zhiqing, Fan Junyan, Liang Liang. *Tool Engineering*[J], 2020, 54(3): 24 (in Chinese)

24 Gao Qi, Gong Yadong, Zhou Yunguang. *China Mechanical Engineering*[J], 2016, 27(6): 801 (in Chinese)

25 Jiang Zhongnan. *Macro-Micro Simulation Analysis on Laser Assisted Cutting of Beryllium*[D]. Harbin: Harbin University of Science and Technology, 2021 (in Chinese)

26 Luo Liang, Yang Xiaojing, Liu Ning *et al*. *Rare Metal Materials*

and Engineering[J], 2019, 48(4): 1130 (in Chinese)
27 Chavoshi S Z, Luo X C. *Materials Science and Engineering A*[J], 2016, 654(1): 400
28 Chavoshi S Z, Luo X C. *RSC Advances*[J], 2016, 6(75): 71409
29 Shao Zihao. *Molecular Dynamics Study on Nano-cutting Deformation Behavior of Monocrystalline γ-TiAl Alloy*[D]. Lanzhou: Lanzhou University of Technology, 2021 (in Chinese)
30 Frenkel D, Smit B, Ratner M A. *Physics Today*[J], 1997, 50(7): 66
31 Plimpton S. *Journal of Computational Physics*[J], 1995, 117(1): 1
32 Stukowski A. *Modelling and Simulation in Materials and Engineering*[J], 2010, 18(1): 2154
33 Tersoff J. *Physical Review B*[J], 1994, 49(23): 16349
34 Purja P G P, Mishin Y. *Philosophical Magazine*[J], 2009, 89(34–36): 3245
35 Ma Yuping, Wei Chao, Zhang Yao *et al*. *China Surface Engineering*[J], 2019, 32(3): 1 (in Chinese)
36 Zhao Xianggang, Hao Xiuqing, Yue Caixu *et al*. *China Surface Engineering*[J], 2022, 35(1): 34 (in Chinese)
37 Wang Shi. *Research on Thermal Stability of Diamond and Thermal Damages of Its Tools*[D]. Dalian: Dalian University of Technology, 2003 (in Chinese)
38 Guo Zhimeng. *Superhard Materials and Tools*[M]. Beijing: Metallurgical Industry Press, 1996 (in Chinese)

MD模拟加载温度对Ni_3Al基合金加工表面的影响

靳　岚[1,2]，李开强[1,2]，伊廷华[1,2]
(1. 兰州理工大学 机电工程学院，甘肃 兰州 730050)
(2. 兰州理工大学 有色冶金新装备教育部工程研究中心，甘肃 兰州 730050)

摘　要：为改善Ni_3Al基合金的纳米切削表面质量以获得更好的服役状态，结合纳米级分子动力学模拟和微观切削实验，探讨了加载温度（300~1050 K）与切削力、表面形貌的关联性。分子动力学模拟结果显示，在纳米切削Ni_3Al基合金过程中，加载温度为750 K时的切削力波动相对于其他温度最小；当加载温度在600~750 K时，影响表面形貌的凸起原子数量最少，即表明加载温度为750 K左右时，Ni_3Al基合金可以获得较高的表面质量。Ni_3Al基合金微观切削实验表明，当加载温度在600~750 K时，加工表面轮廓可以获得较高的平整度，间接验证了在Ni_3Al基合金纳米切削的分子动力学仿真结果的可行性。研究结果表明，选取合适的加载温度是改善Ni_3Al基合金纳米切削加工表面质量的有效途径。

关键词：Ni_3Al基合金；纳米切削；加工表面；加载温度；分子动力学仿真；微观切削实验

作者简介：靳　岚，女，1972年生，博士，副教授，兰州理工大学机电工程学院，甘肃 兰州 730050，E-mail：lan_jane@lut.edu.cn